

$N$	$X_p$	$r$
2	716	$0.0368 \pm 8 \cdot 10^{-4}$
3	471	$0.0242 \pm 5 \cdot 10^{-4}$
4	344	$0.0177 \pm 4 \cdot 10^{-4}$
5	310	$0.0159 \pm 4 \cdot 10^{-4}$
6	290	$0.0149 \pm 4 \cdot 10^{-4}$
7	276	$0.0142 \pm 4 \cdot 10^{-4}$
8	265	$0.0136 \pm 4 \cdot 10^{-4}$
9	256	$0.0131 \pm 4 \cdot 10^{-4}$
10	248	$0.0127 \pm 4 \cdot 10^{-4}$
11	242	$0.0124 \pm 4 \cdot 10^{-4}$
12	237	$0.0122 \pm 3 \cdot 10^{-4}$
13	231	$0.0119 \pm 3 \cdot 10^{-4}$
14	227	$0.0117 \pm 3 \cdot 10^{-4}$

not  
needed.

Table 7. The fringes that intersect at  $90^\circ$  from the vertical axis and their pixel radial distance,  $X_p$ , measured from the holes center. The radial distance,  $r$ , is the converted pixel radial distances using the pixel conversion constant from table 6.

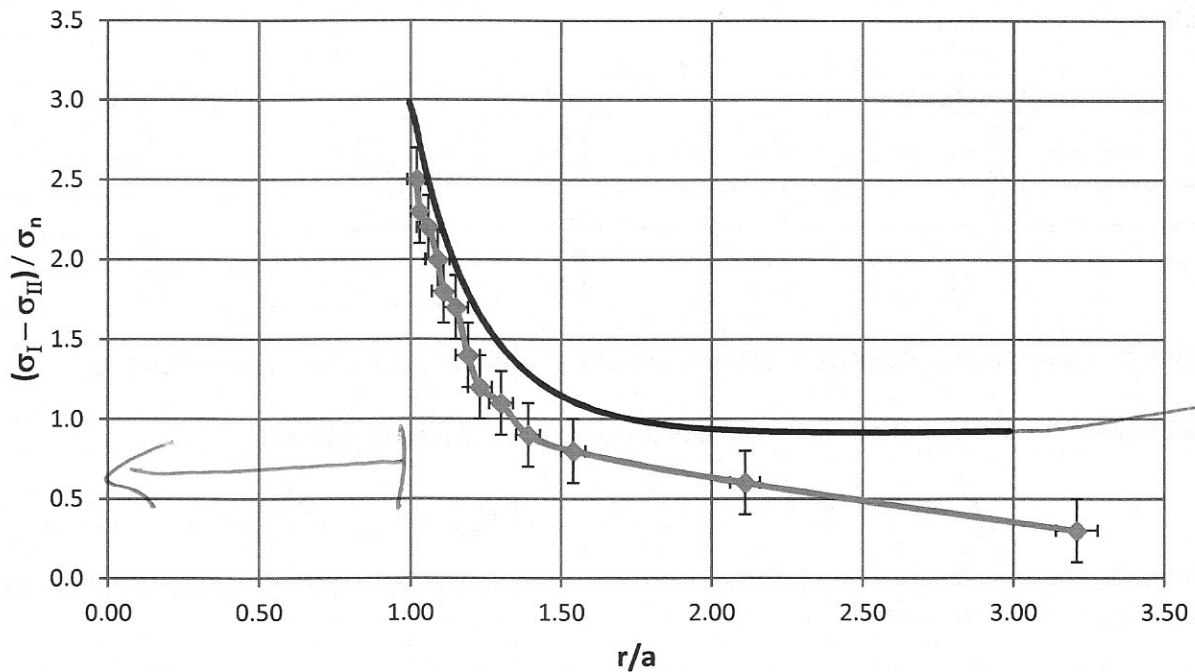


Figure 6. A comparison of the normalized stress from the radius of the holes along the horizontal radial direction at  $90^\circ$  from the vertical plotted in blue versus the normalized theoretical principle stress plotted by black line. The stress concentration,  $S_c$ , is  $2.5 \pm 0.2$ . The error bars indicate the uncertainty in the normalized stress and the normalized location at which the stress is located from the edge of the hole.